

PACS numbers: 42.62.Cf; 42.30.Wb; 05.10.Ln
DOI: 10.1070/QE2006v036n02ABEH013121

Characterisation of optically cleared paper by optical coherence tomography

T. Fabritius, E. Alarousu, T. Prykäri, J. Hast, R. Myllylä

Abstract. **Due to the highly light scattering nature of paper, the imaging depth of optical methods such as optical coherence tomography (OCT) is limited. In this work, we study the effect of refractive index matching on improving the imaging depth of OCT in paper. To this end, four different refractive index matching liquids (ethanol, 1-pentanol, glycerol and benzyl alcohol) with a refraction index between 1.359 and 1.538 were used in experiments. Low coherent light transmission was studied in commercial copy paper sheets, and the results indicate that benzyl alcohol offers the best improvement in imaging depth, while also being sufficiently stable for the intended purpose. Constructed cross-sectional images demonstrate visually that the imaging depth of OCT is considerably improved by optical clearing. Both surfaces of paper sheets can be detected along with information about the sheet's inner structure.**

Keywords: *light coherence, light transmittance, optical length, optical coherence tomography, refraction index mismatch, imaging depth, paper testing, optical clearing agent.*

1. Introduction

Paper consists of a stochastic network of fibers, but since these fibers are much longer than the thickness of the paper sheet, the network can be treated as planar and almost two-dimensional. This two-dimensional structure can be used to determine a number of parameters, and indirectly it even reveals some of the paper's three-dimensional characteristics. However, to improve paper quality, it is important to know its three-dimensional porous structure [1]. Hitherto, research on paper structure has suffered from an absence of nondestructive, fast and cost-effective measurement techniques for micro and macrostructure imaging. Traditional methods are based on ultrasonic, X-ray and magnetic resonance imaging techniques [2 – 4], but in recent years, the availability of reasonably cost-effective lasers has launched the development of optical ranging and imaging methods like low coherence interferometry (LCI), optical coherence tomography (OCT), optical coherence microscopy (OCM) and confocal laser scanning microscopy (CLSM). Optical techniques have been used for structural imaging in medicine for years, but industrial applications are few, because the complex propagation of light inside a scattering medium, such as paper, results in coherent multiple-scattering processes that degrade resolution and image contrast [5 – 10].

From the optical point of view, paper can be categorised as a highly scattering anisotropic medium. In practice, this means that, with a paper thickness of 0.1 mm, the average propagation length of light travelling through a paper sheet is approximately 1 – 10 mm. Since this zigzag path encompasses a number of refraction events, this light will be strongly scattered. In the OCT method, information is derived mostly from single-backscattered photons. Unfortunately, their amount decreases as the imaging depth increases. Thus, the applicability of the OCT method is often unsatisfactory in the depth direction and is usually limited for highly scattering media to 1 – 2 mm [1, 11 – 13].

The aim of this study was to test whether OCT can be efficiently used for paper studies and to find a suitable refractive index matching liquid for paper and to demonstrate experimentally that, as in medical applications, the addition of a clearing agent significantly improves the imaging depth offered by OCT.

2. Optical coherence tomography

Optical coherence tomography (OCT) is a cross-sectional imaging technology, which uses a low coherence optical source to perform reflectometry measurements of the microstructures of materials. OCT utilises an interferometer to measure light reflected from scattering structures with high spatial resolution (< 10 μm) and sensitivity (> 100 dB). The method was originally developed for imaging such biological tissues as the eye and skin as well as various types of skin tumors [6, 14 – 17]. Later, the same technique was also applied to the study of other materials.

Figure 1 presents a simplified version of a typical open-space Michelson interferometer and introduces the notations used troughout this text. The interferometer is illuminated by a near-infrared low temporal coherent light source with Gaussian-shaped emission spectra. Rather than a single frequency, this light source comprises a finite bandwidth of frequencies [18], and its field is split in the interferometer into a reference field E_R and a sample field E_S. A reference mirror is moved at a constant speed v_R to

T. Fabritius, E. Alarousu, T. Prykäri, J. Hast, R. Myllylä Department of Electrical and Information Engineering, Optoelectronics and Measurement Techniques Laboratory, University of Oulu, P.O. Box 4500, 90014 Oulu, Finland; e-mail: tapio.fabritius@ee.oulu.fi

Received Received 19 August 2005; revision received 27 October 2005
Kvantovaya Elektronika **36** (2) 181 – 187 (2006)
Submitted in English

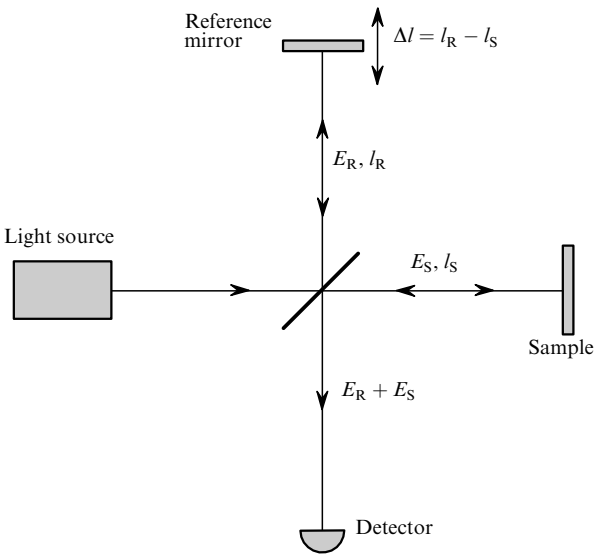

Figure 1. Michelson interferometer.

produce interference modulation at the Doppler frequency for optical heterodyne detection,

$$f_D = \frac{2v_R}{\bar{\lambda}} \tag{1}$$

where $\bar{\lambda}$ is the mean wavelength of the source. Shifting the interference signal to the Doppler frequency facilitates the removal of dc background and low-frequency noise during demodulation [6]. Backscattered light from the object is then recombined by a detector with the light reflected from the reference mirror. As mentioned earlier, a coherent interference signal is evident at the detector only when the reference arm distance matches the optical length of the reflective path through the object to within the coherence length of the source,

$$L_c = \frac{2\ln 2}{\pi}\frac{\bar{\lambda}^2}{\Delta\lambda}, \tag{2}$$

where $\Delta\lambda$ is the spectral FWHM (full width at half-maximum) of the light source. The selection of photons is performed by the optical path length, which inevitably causes distortion in signal derived from highly scattering medium due to the influence of multiple scattering of photons [19, 20].

The distances measured by the OCT are always optical distances and must be scaled by the group refractive index n_g of the medium,

$$n_g = n - \lambda\frac{dn}{d\lambda}, \tag{3}$$

where n is the refractive index of the medium. In real materials, not only the refractive index n is a function of wavelength, but also the group index n_g. The result is a broadening of the interferograms and an increase in coherence length, leading to a corresponding reduction in resolution. In dispersive media, the coherence length $L_{c,m}$ can be calculated by

$$L_{c,m} = \left[L_c^2 + \left(\frac{dn_g}{d\lambda}d_g\Delta\lambda\right)^2\right]^{1/2}, \tag{4}$$

where d_g is the geometric depth of the media. Hence, resolution within dispersive media can be stated as $L_{c,m}$ [21–22].

The interferometer functions as a cross-correlator and the detected intensity at the detector is given by

$$I_d(l_S, l_R) = I_S + I_R + \sqrt{2I_R I_S}\int_{-\infty}^{\infty}\sqrt{R(l_S)}|V_{tc}(\Delta l)|\cos\bar{k}\Delta l\,dl_S, \tag{5}$$

where l_S and l_R are the optical path lengths in the sample and the reference arm, respectively; I_S is the detected intensity backscattered by the sample; and I_R is the detected intensity reflected by the reference mirror. In Eqn (5), $\sqrt{R(l_S)}$ acts as normalised path-length-resolved reflectance or normalised derivative from the intensity depth distribution of the measuring wave, representing the fraction of power reflected from the layer located at position l_S within the object. Further, $V_{tc}(\Delta l)$ is the temporal coherence function, i.e., a Fourier transform of the power spectral density of the light source; Δl is the optical path difference $|l_S - l_R|$ between the reference and the sample arm; and $\bar{k}$ is the average wave number $2\pi/\bar{\lambda}$. Thus, the interference modulation can be rewritten as

$$\tilde{I}_d(l_S, l_R) = 2\sqrt{I_S I_R}\left(\sqrt{R(l_S)}\otimes C(l_S, l_R)\right), \tag{6}$$

where $C(l_S, l_R)$ is the interferometer response in the ideal case with a mirror in both arms. In short, OCT traces out local relative variations in path-length resolved reflectance induced by local inhomogeneities in an object's optical properties, including the refractive index Δn, scattering coefficient $\Delta\mu_S$, anisotropy Δg or absorption coefficient $\Delta\mu_a$ [5, 6, 22–25].

3. Refractive-index matching

Influential early studies and theories on the propagation of light in paper include those by Kubelka & Munk and Scallan & Borch [26, 27]. Since then, other researchers have presented more sophisticated models [28, 29]. One of the biggest problems afflicting models for evaluating the optical properties of paper is that some of the optical parameters of paper components are not known. In addition, the relationship between optical backscattering and total attenuation is very complex, and most models fail to account for the physical and chemical changes that occur during these processes. As a result, theoretical models only provide general information about optical phenomena in paper wetted with a refractive index matching liquid.

In a dry paper sheet, light scatters at the air–solid interface. Assuming that all the components of paper have similar refraction indices (cellulose $n_c = 1.55$), total light scattering is a function of the air–solid interface. However, due to the significant difference between the refractive indices of cellulose and air ($n_0 = 1$) [13], the transmission of light in dry paper is debased. When a refractive index matching liquid is used, paper pores are filled with a solute, whose refraction index is larger than that of air. This serves to reduce the refraction index mismatch, thereby enhancing the light penetration depth. In medical applications of OCT, refractive index matching liquids such as glucose and

glycerol are used to improve the light penetration properties of the tissues under study [30–36].

The ability of paper to transmit light depends on the absorption coefficient (μ_a), scattering coefficient (μ_s) and anisotropy factor g. In dry paper, $\mu_a \ll \mu_s$ and, therefore, the improved transmittance of optically cleared paper is a consequence of the reduced effective scattering coefficient $\mu'_s = (1-g)\mu_s$. Degrading the effective scattering coefficient improves the probability of recording photons carrying important information about the inner structure of paper using OCT [33].

In this work, four different liquids were selected for optical 'clearing' of paper. As previous studies have demonstrated, the structural properties of paper can be determined by OCT. The surface properties can be easily evaluated by low coherence interferometry (LCI) but structural OCT imaging of paper needs more sophisticated methods [37]. The optical clearing of paper to enhance its optical properties for OCT imaging was introduced by Alarousu et al. in 2005 [38]. This is important, since, although the surface profile of paper is informative as such, many prominent characteristics, such as wettability, strength and brightness, are partially determined by the paper's 3D structure.

4. Measurement system

In this study, evaluations concerning the transmittance and stability of transmitted light were based on transmitted light power measurements. As shown in Fig. 2, the measurement setup, placed in the vertical direction, utilised a superluminescent diode (SLD) with a central wavelength of 831.9 nm as a light source. The output power of the SLD was 600 μW. A pinhole was used to decrease the radius of the collimated spot size to 1 mm. Underneath the sample was a light detector, connected to an output signal power measurement device (Ando AQ2140) with a sampling frequency of 1 Hz.

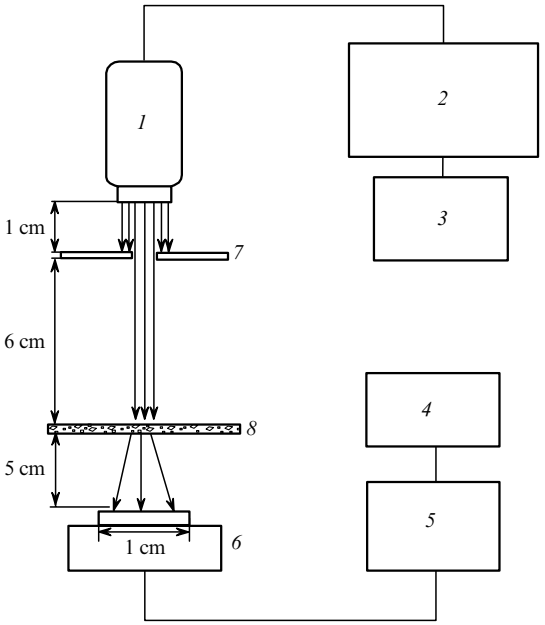

Figure 2. Schematic of the setup used in the light transmission measurement: (*1*) SLD; (*2*) current and temperature controller; (*3*) power supply; (*4*) computer; (*5*) Ando AQ2140 optical multimeter; (*6*) detector; (*7*) pinhole; (*8*) sample.

At the core of the used OCT system is a Michelson-type interferometer in a free space configuration.

A schematic of the OCT system, presented in Fig. 3, shows that the setup uses a superluminescent diode delivering a peak output power of 50 mW at a central wavelength of 831.9 nm with a spectral FWHM of 19.7 nm. In free space, the axial resolution provided by the light source is 15.5 μm. More detailed description of the device can be found from previous article of the group [38]. Imaging was performed by directing a low-coherence light at the sample and using a pietzoelectric-scanning system to detect reflections from the internal structures of paper. Transverse scanning was accomplished by synchronised, computer-controlled, step motors. Transverse light-beam diameter is 15 μm in the object plane, which is produced from collimated light beam using diode laser optics.

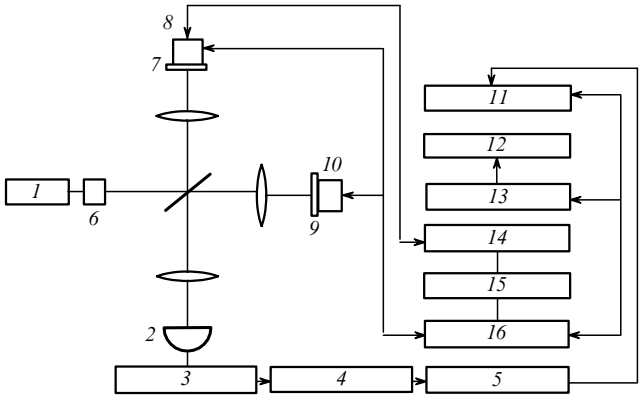

Figure 3. Schematic of the OCT system: (*1*) SLD; (*2*) photodiode; (*3*) preamplifier; (*4*) bandpass filter; (*5*) demulator; (*6*) collimator; (*7*) mirror; (*8*) axial scanner; (*9*) sample; (*10*) lateral scanner; (*11*) data acquisition; (*12*) display; (*13*) computer; (*14*) PZT driver; (*15*) ramp generator; (*16*) motion controller.

5. Materials and methods

To examine and compare the dependence of light transmittance on the individual properties of specific refractive index matching liquids, we used copy paper sheets (Optitext) with a basis weight of 80 g m^{-2} and a thickness of 102 μm. Exact information about the fillers and sizing agents of the sheets were not available that is usual with commercial paper samples. Our measurements were performed on separate sheets, because certain refractive index matching liquids cause irreversible effects on the physical and chemical properties of the sheets.

Selection of refractive index matching liquids was based on the fact that the refractive indexes of ethanol, 1-pentanol, glycerol (85 % and pure) and benzyl alcohol increase almost linearly between 1.36–1.54, as shown in Table 1 [39]. In

Table 1. Refractive indexes of used clearing agents.

Agent	Refractive index
Air	1.000
Ethanol	1.359
1-Pentanol	1.407
Glycerol (pure)	1.474
Benzyl alcohol	1.538

addition, liquids were selected so that they have refractive index nearby paper's refractive index and being as stabile as possible. The exact refractive index of glycerol (85 %) was not known. Glycerol (85 %) contains 15 % water and was used to demonstrate how the optical and physical properties of a liquid change as its polarity increases. In the experiments aimed at evaluating the transmission of light, a small volume of liquid (3 μL) was applied with a pipette and shot to the surface (4 cm^2) with a pneumatic sprayer. For OCT imaging, the samples were totally wetted and excess liquid was removed.

The OCT measurement was essentially a conventional point to point measurement. The size of the 2D cross sections are 1×0.316 mm (here and below optical sizes are used, i.e., $l = l_0 n$, where l_0 is the geometrical size), while 3D image covers a space of $0.75 \times 0.75 \times 0.16$ mm. The measurement time of the 2D cross section was 1min 40 s and 3D image 21 min. The 2D cross sections and 3D image were constructed by using built-in Matlab™ image tools and 3D rendering algorithms and moderate 2D and 3D median filtering were used for image enhancement.

Both measurement systems were placed in an optical measurement table to reduce vibration effects. In addition, the setup in the light transmission measurement was covered with a non-transparent box for the duration of the experiment to eliminate harmful effects produced by the background light.

6. Results

6.1 Light transmittance measurements

OCT imaging is a time-consuming process, because OCT images are constructed from point to point manner. Investigating the time dependence of light transmittance is necessary, because OCT measurements require a sufficient amount of a stable clearing agent. Moreover, for a successful measurement, the refractive index matching liquid's evaporation rate has to be relatively slow. Needless to say, all processes that change the structure of paper are not desired. The intensity level between separate measurements is affected by the stochastic structure of the paper and differences in the way the liquid spreads on its surface. Thus, Figure 4 presents the results in a normalised form.

Light transmittance measurements for different refractive index matching liquids provided the information concerning the penetration of light into paper. According to our measurements, benzyl alcohol has the largest effect on light transmittance. Thus, light penetrates about 2 times better into paper wetted with benzyl alcohol than into dry paper (Fig. 4). The maximum transmittance of benzyl alcohol was 2.01, while the corresponding value for 1-pentanol was 1.91, for glycerol (85 %) – 1.76 and for ethanol – 1.77. A sample wetted with pure glycerol, however, failed to achieve its maximum transmittance value during the 12-minute measurement.

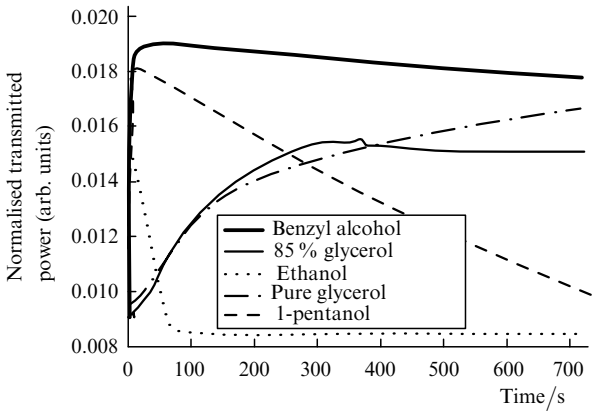

Figure 4. Time dependence of light transmittance. At zero, the clearing agent was applied.

These paper measurements further demonstrated that, in terms of stability, the most salient characteristics are liquid sorption and evaporation. The sorption process for pure glycerol is really slow, and the maximum transmittance value could not be achieved in 12 minutes. Nevertheless, when the glycerol was diluted by water sorption, this velocity increased. Consequently, glycerol wetted paper (85 %) achieved its maximum light transmittance value in 6 minutes, which suggests that some of the applied refractive index matching liquid were sorpted. Transmittance measurements, combined with a visual examination of glycerol (85 %) wetted paper, proved that certain structural changes take place in about 6 minutes from the beginning of the measurement. Finally, as shown by Fig 4., ethanol, 1-pentanol and benzyl alcohol all seem to wet pores and cavities at a similar velocity.

The figure also indicates that the transmittance of glycerol (85 %) wetted paper does not change after 9 minutes, although some kind of saturation value can be observed in the case of pure glycerol. However, this saturation time is much longer than 12 minutes. Ethanol, on the other hand, evaporated from the sample in 3 minutes and 1-pentanol in 15 min. The light transmittance of paper wetted with benzyl alcohol decreased only by 8 % during 12 minutes, meaning that the evaporated volume of the refractive index matching liquid was very small. Linear extrapolation suggests that the evaporation of (3 μL) benzyl alcohol takes over 1 hour and 30 minutes. In practise, the evaporation time is even longer than that.

6.2 OCT measurements

Our transmittance measurements proved that, as refractive index matching liquids, ethanol and glycerol (85 % and pure) are unsuitable for paper characterisation with an OCT system. Due to ethanol's and glycerol's inefficacious sorption and evaporation properties, the obtained tomography pictures are largely irrelevant. Nevertheless, to prove the enhancement in imaging depth provided by 1-pentanol and benzyl alcohol, dry paper with a thickness of 102 μm and a width of 1 mm was measured. Figure 5 shows the constructed 2D tomography pictures.

The constructed cross section profile for dry copy paper demonstrates a case, where the imaging depth of OCT is not adequate. As the scanning depth of the used OCT system was limited, the constructed cross section profile for dry paper seems to cut away (Fig. 5a). In reality, however, the signal will fade away in the same way as in the sample representing 1-pentanol (Fig. 5b), where the bottom surface of the paper is unclear. Although paper wetted with 1-pentanol transmits much more light than dry paper, the imaging depth is still insufficient. A proper image of the sheet's bottom surface can only be obtained with benzyl alcohol (Fig. 5c). Reflectance from the top and bottom surface of a paper sheet wetted with benzyl alcohol was

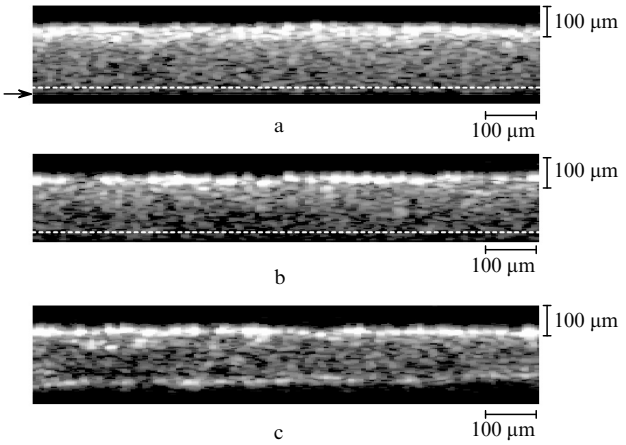

Figure 5. Constructed 2D images of the used paper samples: (a) dry paper, paper wetted with (b) 1-pentanol, (c) benzyl alcohol. In the lateral and depth direction, the pixel size of the images is 15 μm and 0.39 μm, respectively. Black arrow is pointing the scanning depth limit of the used measurement system. The white dashed line presents estimation of the rear border of paper.

equal. Light scattering and absorption, however, attenuates the reflected intensity from the bottom surface.

The 3D image shown in Fig. 6 indicates that the inner structures of paper sheets can be determined with OCT. In fact, such cross section profiles seem to include characteristics similar to those seen in corresponding images obtained by other techniques (X-ray, SEM, etc.) [3, 39]. Since the diameter of the smallest pores in paper measures only a couple of nanometres, the determination of the smallest observable structural component is restricted by the OCT system's resolution. Typical wood based fibres are about 1 – 4 mm in length, and as their thickness is 30 – 100 times smaller than their length [1], the dimensions of single fibers are within OCT's detection range.

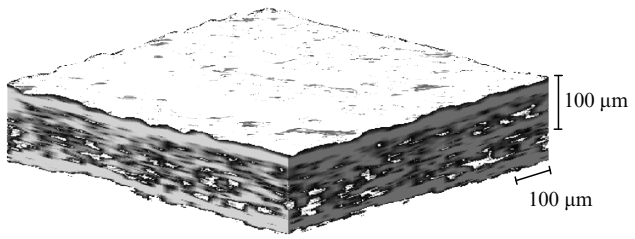

Figure 6. Constructed 3D-image of copy paper. The size of the image is $0.75 \times 0.75 \times 0.16$ mm (optical). The pixel size in lateral direction is 15 μm and in depth direction 0.39 μm.

7. Discussion

7.1 Suitable clearing agent for OCT measurements

Our light transmission measurements involved applying a small volume (3 μL) of refractive index matching liquid into paper samples. All samples were partially wetted, in other words, they contained both air and agent filled gaps. A non-linear relationship exists between transmittance and the total attenuation coefficient; therefore, partial wetting entails a smaller improvement in transmission capability. This explains why the maximum improvement in light transmittance does not vary significantly between the different agents shown in Fig. 4. Nevertheless, preliminary studies have suggested that, for example, paper that is totally wetted with benzyl alcohol transmits light over a dozen times better than paper soaked in ethanol.

Further, our experimental results suggest that the largest improvement in transmittance is achieved, when the refraction index of the applied refractive index matching liquid closely matches that of the paper sheet. The results also bear out the supposition that refractive index matching liquids reduce scattering as a result of better refraction index matching with the ground medium. A similar finding has been reported in the medical application of OCT [17].

Because the refraction index of benzyl alcohol is quite similar to those of cellulose (1.55) and typical fillers (Calcium Carbonate $\sim$1.6; Clay $\sim$1.6), the improvement in transmittance is significant. The maximum transmission improvement for glycerol (85%) should exceed that for ethanol, because the former offers better refraction index matching. Surprisingly, as seen in Fig. 4, light is transmitted better in ethanol. A visual evaluation of the paper sheet combined with the irregular behaviour of the transmittance curve of glycerol (85 %) (6 minutes after the beginning of the sorption process) indicate that 85 % glycerol causes the paper to curl, thereby reducing its transmittance capacity. When paper is wetted, the liquid penetrates into its pores. The swelling takes place when a polar liquid, such as water, interacts with paper [12]. The paper volume increases on swelling, because the molecules of the liquid penetrate between hydrogen bonded fibrils in the fiber wall [27]. As a consequence, paper swelling reduces OCT's imaging depth. This observation suggests that ethanol and glycerol are not useful refractive index matching liquids in paper characterisation.

Owing to the low sampling frequency of the used light transmission measurement system, it was impossible to detect differences between the sorption properties of ethanol, 1-pentanol and benzyl alcohol. Although the sorption velocity of paper is not an essential characteristic in OCT measurements, fastness offers an advantage, since it does away with the need to control the sorption time of the used agent.

OCT images are made in point to point manner and the measurements may take several dozens of minutes. If the evaporation rate of the used refractive index matching liquid is significantly high, imaging depth is reduced during the measurement period, with a corresponding loss in the amount of available information concerning the paper's inner structure. Of the agents used in our experiments, ethanol, 1-pentanol and benzyl alcohol all evaporate, and the transmission measurements demonstrated clearly that ethanol's evaporation rate is too high for our purposes. The evaporation velocity of benzyl alcohol seems to be lower than that of 1-pentanol, making it more suitable for paper measurements. Glycerol (pure and 85 %), on the other hand, evaporates at such a slow pace as to make evaporation insignificant in the measurement conditions described here. It must be borne in mind, however, that due to its previously discussed properties, glycerol is unsuitable for studying copy paper.

7.2 Effect of optical clearing on imaging depth

As the constructed cross section OCT images suggest, the only refractive index matching liquid that produces a

sufficient improvement in imaging depth is benzyl alcohol. Further, imaging depth in paper wetted with either ethanol or glycerol is too small for practical use. Additionally, the use of a refractive index matching liquid changes the scattering properties of paper. Unfortunately, an effective method for quantifying the imaging depth of OCT in paper measurements has yet to be found.

We assumed above that paper is composed of components (cellulose) with similar refractive indices. If we also hypothesise that the refraction index of the clearing agent equals that of cellulose, only the top and bottom surface of paper sheets can be characterized. As the copy paper samples used here consisted of fibres, fillers and sizing agents, their structure is more complex. However, using a sizing agent serves to increase the sample's heterogeneity, which enables an evaluation also of the inner structural components of paper – even when the refraction index of the refractive index matching liquid closely matches that of the paper.

Using a more sophisticated data processing method, combined cross section profiles can be used to create three dimensional paper structures. This implies that the method presented here can also be used to determine the porosity of paper, which is one of its most important characteristics [8]. Earlier methods for the characterisation of the three dimensional structure of paper, including confocal laser scanning microscopy (CLSM) and X-ray imaging, have some drawbacks. CLSM suffers from inadequate imaging depth, while X-ray imaging is expensive [3]. As for the OCT method discussed in this paper, problems such as these are not an impediment, provided that a suitable clearing agent is used.

8. Conclusions

Light transmission measurements in paper established that the sorption and evaporation behaviour of ethanol and glycerol were impractical for optical coherence tomography measurements. Minimising the refraction index mismatch to reduce the coherent multiple light scattering by optical clearing agent doesn't completely depend on optical properties of used agent but also its sorption and evaporation characteristics when added in paper. Ethanol evaporated too fast and glycerol (85 % and pure) was sorpted too slowly. In addition, the sorption process also produced irreversible structural changes. Both 1-pentanol and benzyl alcohol had suitable sorption properties, but only benzyl alcohol offered a sufficiently good OCT imaging depth. The evaporation rate of benzyl alcohol was several dozen times longer than that of 1-pentanol, and it also boasted a greater improvement in light transmittance. As a result, benzyl alcohol was deemed as the most suitable clearing agent for optical measurements.

Better light penetration increases the imaging depth of OCT and enables the detection of the top and bottom surface of paper sheets. It should be noted that an evaluation of the inner structure of paper depends on the resolution provided by the OCT system. The method presented in this paper also allows obtaining information about the three dimensional structure of paper and the evaporation of the used refractive index matching liquid. This paper also succeeded in determining the most appropriate clearing agent for optical measurements on paper. Taking account of the useful properties of OCT opens a range of new avenues of research for paper testing and the paper-making industry.

References

1. Niskanen K. *Paper Physics, Papermaking Science and Technol.* (Jyväskylä: Fapet Oy, 1998) Vol. 16.
2. http://www.ind.tno.nl/en/cost action e11/index.html
3. Samuelsen E.J., Gregersen O.W., Houen P.J., Helle T., Raven C., Snigirev A. *J. Pulp and Paper Sci.*, **27**, 50 (2001).
4. Häggkvist M. *Licentiate Thesis* (Stockholm: Kungl. Tekniska Högskola, Royal Ins. of Technol., 1999).
5. Pan Y., Birngruber R., Rosperich J., Engelhart R. *App. Opt.*, **34**, 6564 (1995).
6. Schmitt J.M. *IEEE J. Sel. Top. Quantum Electron.*, **5**, 1205 (1999).
7. Alarousu E., Myllylä R., Gurov I., Hast J. *Proc. SPIE Int. Soc. Opt. Eng.*, **4595**, 223 (2001).
8. Bestemyanov K.P., Gordienko V.M.., Konovalov A.N., Podshivalov A.A. *Proc. SPIE Int. Soc. Opt. Eng.*, **5475**, 56 (2004).
9. Zimnyakov D.A., Zakharov P.V., Trifonov V.A., Chanilov O.I. *JETP Lett.*, **74** (4), 216 (2001).
10. Zakharov P.V. Zimnyakov A.A. *Tech. Phys. Lett.*, **28** (12), 1015 (2002).
11. Carlsson J., Hellentin P., Malmqvist L., Persson A., Persson W., Wahlstrom, C.-G. *App. Opt.*, **34**, 1550 (1995).
12. Lyne B. *Handbook of Physical Testing of Paper* (New York: Marcel Dekker Inc., 2001).
13. Karppinen T., Kassamakov I., Haeggström E., Sorvonen-Pellinen J. *Meas. Sci. & Tech.*, **15**, 1223 (2004).
14. Huang D., Swanson E.A., Lin C.P., Shuman J.S., Stinson W.G., Chang W., Hee M.R., Flotte T., Gregory K., Puliafito C.A., Fujimoto J.G. *Science*, **254**, 1178 (1991).
15. Brezinski M.E., Fujimoto J.G. *IEEE J. Sel. Top. Quantum Electron.*, **5**, 1185 (1999).
16. De Boer J.F., Srinivas S.M., Hyle Park B., Pham T.H., Chen Z., Milner T., Nelson J.S. *IEEE J. Sel. Top. Quantum Electron.*, **5**, 1200 (1999).
17. Tuchin V.V., Xu X., Wang R.K. *App. Opt.*, **41**, 258 (2002).
18. Bourma B.E., Tearney G.J. *Handbook of Optical Coherence Tomography* (Switzerland: Marcel Dekker Inc., 2002).
19. Bestem'yanov K.P., Gordienko V.M., Ivanov A.A., Konovalov A.N., Podshivalov A.A. *Kvantovaya Elektron.*, **34** (7), 666 (2004) [*Quantum Electron.*, **34** (7), 666 (2004)].
20. Hitzenberger C.K., Drexler W., Baumgartner A., Fercher A.F. *Proc. SPIE Int. Soc. Opt. Eng.*, **2981**, 29 (1997).
21. Hitzenberger C.K., Drexler W., Fercher A.F. *Investigative Ophthalmology & Visual Science*, **33**, 98 (1992).
22. Hitzenberger C.K. *Appl. Opt.*, **31** (31), 6637 (1992).
23. Fercher A.F. *J. Biomed. Opt.*, **1**, 157 (1996).
24. Pan Y., Lankenau E., Welzel J., Birngruber R., Engelhardt R. *IEEE J. Select. Top. Quantum. Electron.*, **2**, 1029 (1996).
25. Hast J., Gurov I., Alarousu E., Zakharov A., Myllylä R. *Proc. SPIE Int. Soc. Opt. Eng.*, **5486**, 180 (1994).
26. Kubelka P.S., Munk F. *Z. Techn. Phys.*, **12**, 593 (1931).
27. Scallan M., Borch J. *Tappi J.*, **55**, 583 (1972).
28. Leskelä M. *Paper and Timber*, **75**, 683 (1993).
29. Saarinen K., Muinonen K. *Appl. Opt.*, **40**, 5064 (2001).
30. Chance B., Liu H., Kitai T., Zhang Y. *Anal. Biochem.*, **227**, 351 (1995).
31. Vargas G., Chan E.K., Barton J.K., Rylander H.G., Welch A.J. *Laser Surg. Med.*, **24**, 138 (1999).
32. Wang R.K., Tuchin V.V., Xu X., Elder J.B. *J. Opt. Soc. Am. B*, **18**, 948 (2001).

33. Zimnyakov D.A., Tuchin V.V. *Kvantovaya Elektron.*, **32** (10), 849 (2002) [Quantum Electron., **32** (10), 849 (2002)].
34. Tuchin V.V., Maksimova I.L., Zimnyakov D.A., Kon I.L., Mavlutov A.H., Mishin A.A. *J. Biomed. Opt.*, **2**, 401 (1997).
35. He Y., Wang R.K. *J. Biomed. Opt.*, **9**, 200 (2004).
36. Tuchin V.V. *J. Biomed. Opt.*, **4**, 106 (1999).
37. Alarousu E., Prykäri T., Erkkilä A.-L., Myllylä R., Hast J. *Proc. 4th Topical Meeting on Optoelectronic Distance/Displacement Measurements and Applications* (Oulu, Finland, 2004) pp 36 – 41.
38. Alarousu E., Krehut L., Prykäri T., Myllylä R. *Meas. Sci. Tech.*, **16**, 1131 (2005).
39. Weast R.C. *Handbook of Chemistry and Physics* (Ohio: Chemical Rubber Co., 1966).